Journal of Geophysical Research: Earth Surface

Supporting Information for

Quantification of gravitational mass wasting and controls on submarine scarp morphology along the Roseau fault, Lesser Antilles

Alex Hughes[1], Javier Escartín[2, 1], Jean-Arthur Olive[2], Jeremy Billant[3], Christine Deplus[1], Nathalie Feuillet[1], Frédérique Leclerc[3], Luca Malatesta[4]

1 Université de Paris, Institut de physique du globe de Paris, CNRS, F-75005 Paris, France

2 Laboratoire de Géologie, Ecole Normale Supérieure (CNRS UMR 8538), PSL Research University, Paris, France

3 Université Côte d'Azur, CNRS, Observatoire de la Côte d'Azur, IRD, Géoazur, Valbonne, France

4 GFZ German Research Center for Geosciences, Potsdam, Germany

Contents of this file

Introduction

This supporting information provides additional text (Text S1 and S2) to support methodology for quantifying scarp morphology and erosion described in section 5 of the main manuscript and illustrated in Figure 8 of the main manuscript. Various supplemental figures are also included to support the text in the main manuscript. This supporting information also provides additional tables on the datasets and calculations provided in the main manuscript.

Text S1. Calculations for scarp morphology

We calculated scarp average slope and apparent scarp height from bathymetric profiles extracted from the 1 m/pixel digital terrain model (DTM). Profiles were spaced one meter apart and projected perpendicular to the mean fault strike for the Roseau segment. We identified the top of the scarp (point 1 in Figure 8B) as the inflection point between the dip of the regional seafloor in the footwall and the opposing dip of the fault scarp, which was identified using slope and aspect maps (Figure S4). We defined the hanging wall cut-off (point 3 in Figure 8B) as the topographic break in slope at the base of the fault free face (if present), which we identified in shaded relief or slope maps (Figure S4). If no free face was visible in the 1 m/pixel DTM, we interpreted the base of the scarp as either the transition from footwall erosion to hanging wall deposition based on the surface morphology of the scarp (e.g., the presence of a catchment outlets or a truncation of incisional gullies etc.) and/or the transition from > 30° to < 30° slope. Using these criteria, apparent scarp height was measured upwards from the top of the sediment apron deposited on the hanging wall (vertical distance between points 1 and 2 in Figure 8B), thus excluding the portion of the scarp buried under hanging wall sediment. Scarp average slope was calculated by dividing scarp height by the distance perpendicular to fault strike over which scarp height is measured (horizontal distance between points 2 and 3 in Figure 8B).

Text S2. Volume-balancing calculations

To calculate the volume eroded from footwall catchments, we cropped the 1 m/pixel DTM to the map-view extent of the catchments extracted with TopoToolbox (Schwanghart & Scherler, 2014). We calculated erosion from individual bathymetric profiles extracted from the 1 m/pixel DTM, spaced 1 m apart, and oriented perpendicular to fault strike at the catchment outlet over the entire footprint of the catchment.

The calculation of erosion from the bathymetric profiles requires a projection of the fault dip (projection from point 3 to 4 in Figure 8B) and a projection of the seafloor in the footwall of the scarp (projection from point 1 to 4 in Figure 8B). To define the fault dip, we assumed that the slope of the fault free face, imaged in the video-derived three-dimensional terrain models, is a proxy for the fault dip in the shallow subsurface. We measured the slope of the fault free face at thirty-nine locations in fourteen three-dimensional models using the software MESHLAB (Figure S1). We then used the nearest fault dip value from to the catchment of interest as the fault dip projection in our calculations.

We measured an average slope of the footwall dipping away from the scarp ($14° ^{+4}/_{-3}$) using a ~5 km wide transect immediately adjacent to the Roseau fault scarp in the footwall from the 10 m/pixel DTM. We integrated for the area underneath the bathymetry that corresponds to the projection of the uneroded seafloor and the fault free face (i.e., the area between points 1, 2, and 3 in Figure 8B) and subtracted the resulting area from the total area under the projection of the uneroded seafloor and the projection of the fault free face (i.e., the area of the quadrilateral between points 1 through 4 in Figure 8B). The total volume eroded from each catchment is the sum of erosion from each bathymetric profile along strike in the direction of mean fault strike covering the footprint of the catchment. Positive uncertainty was modeled using the maximum dip of the fault free face measured from the three-dimensional models (86°) in combination with the maximum dip of the seafloor in the footwall of the scarp (18°) (Figure 8C). The minimum equivalent values for the dip of the fault free face (59°) and the dip of the seafloor in the footwall (11°) were used for negative uncertainty (Figure 8C).

To calculate the volumes of the debris cones requires a quantification of the distal margin of the cone and the transition from debris cone surface to the seafloor (Figure S5). For cones at southeastern and central sections of the Roseau segment (areas B and C), the distal margin of the cones is clearly visible as an abrupt break in slope in hillslope maps, bathymetric profiles, and slope profiles (Figure S5B). However, the transition from cone surface to seafloor is gradual for debris cones along the northwestern Roseau segment in area A (Figure S5C).

In area A, the seafloor in the hanging wall generally dips less than 5° away from the fault (Figure S5C). Therefore, to map the distal cone margins, we masked the slope maps extracted from the 1 m/pixel DTM to a minimum value of 8° and manually traced the extent of the cropped slope map to delineate the distal boundary of the debris cones (Figure S5E). The minimum value of 8° was selected because this is the minimum slope above the dip of the seafloor that highlights the shape of the distal margin of the cones. Masking the slope maps at 10° underestimates volumes of the smaller cones and masking the slope maps below 8° results in cones that do not resemble radial depositional features. Using the outline of the masked slope maps as a guide, we cropped the 1 m/pixel DTM to the outline of the cone and used the cropped DTM to calculate cone volumes.

To quantify the volume of the debris cones from the cropped DTM, we integrated for the total area under the cone surface (the area between points 3, 5, and 6 in Figure 8B) using bathymetric profiles oriented perpendicular to mean fault strike at the corresponding catchment outlet. As

with the eroded volume calculations, profiles were spaced every meter along the fault and extracted from the 1 m/pixel DTM. The depositional cross-sectional area of each profile is calculated as the triangle set by the average slope of the fault plane, the surface of the cone, and the horizontal projection of the hanging wall floor (triangle 3-6-7 in Figure 8B). The total cone volume is the sum of cross-sectional cone volumes along strike in the direction of mean fault strike at the corresponding catchment outlet.

We calculated positive uncertainty on the cone volumes by assuming that the seafloor in the hanging wall dips 10° towards the fault based on the average gradient of the seafloor on the flanks of the reef plateau (Leclerc et al., 2016) and using the maximum fault dip from the three-dimensional outcrop models of 86° (Figure 8C). We calculated minimum cone volumes using the minimum fault dip from the three-dimensional models of 59° (Figure 8C) and assuming that the seafloor in the hanging wall dips at most 8° away from the fault based on the analysis in Figure S5. We also recorded the average surface slope of the debris cones from the fault to the distal boundary of the debris cone (the average slope of the line between points 3-6 in Figure 8B).

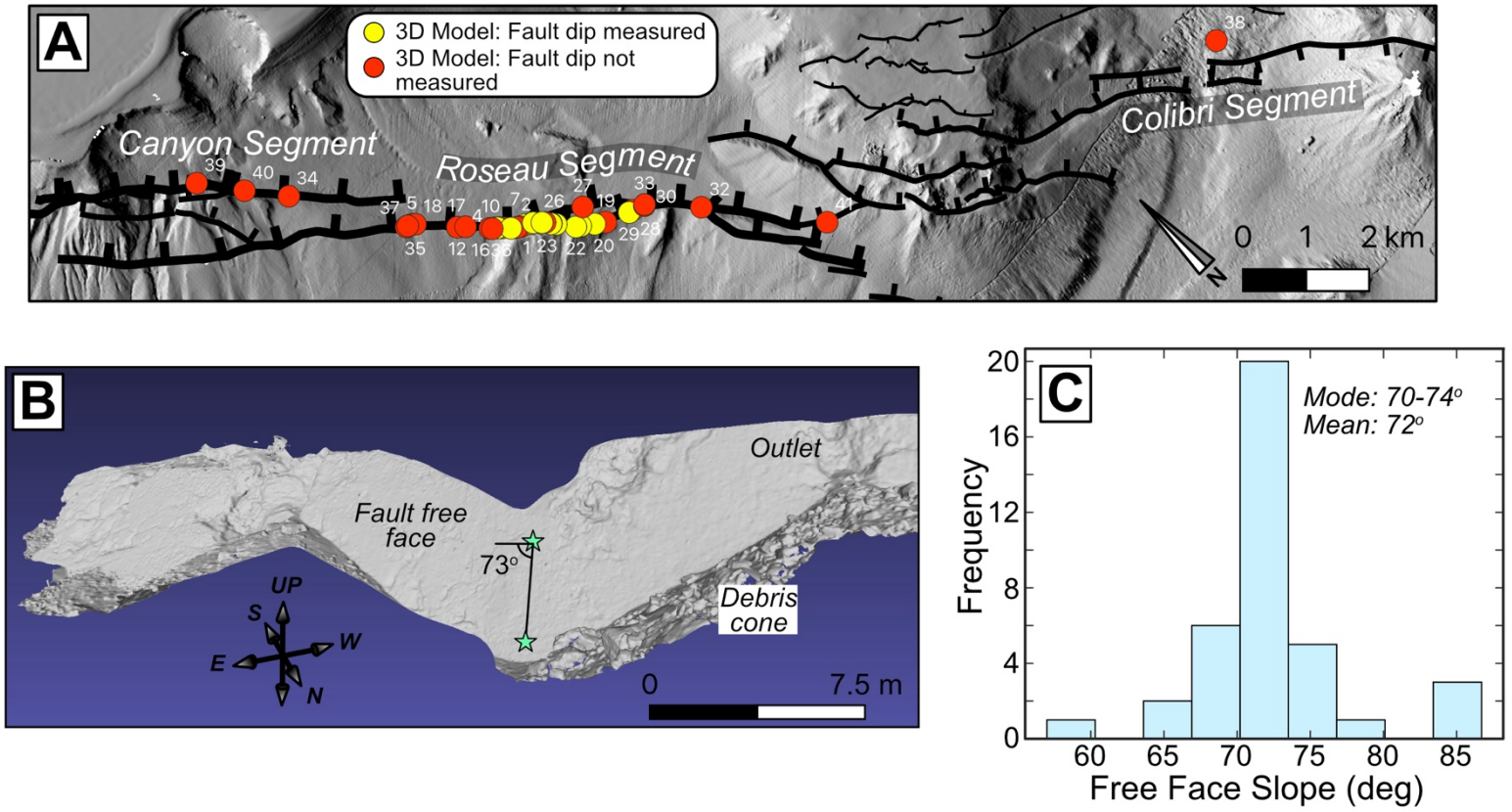

Figure S1. *A) Hillshade map showing the location of the three-dimensional outcrop models referred to in the main manuscript. Numbers next to models refer to the ID in table S2. Location of part A shown in Figure 4A. B) Three-dimensional outcrop model of part of the fault free face in the Roseau segment showing how we calculated fault dip using two points on the plane. C) Histogram showing the distribution of fault dips measured at thirty-eight locations from fourteen models.*

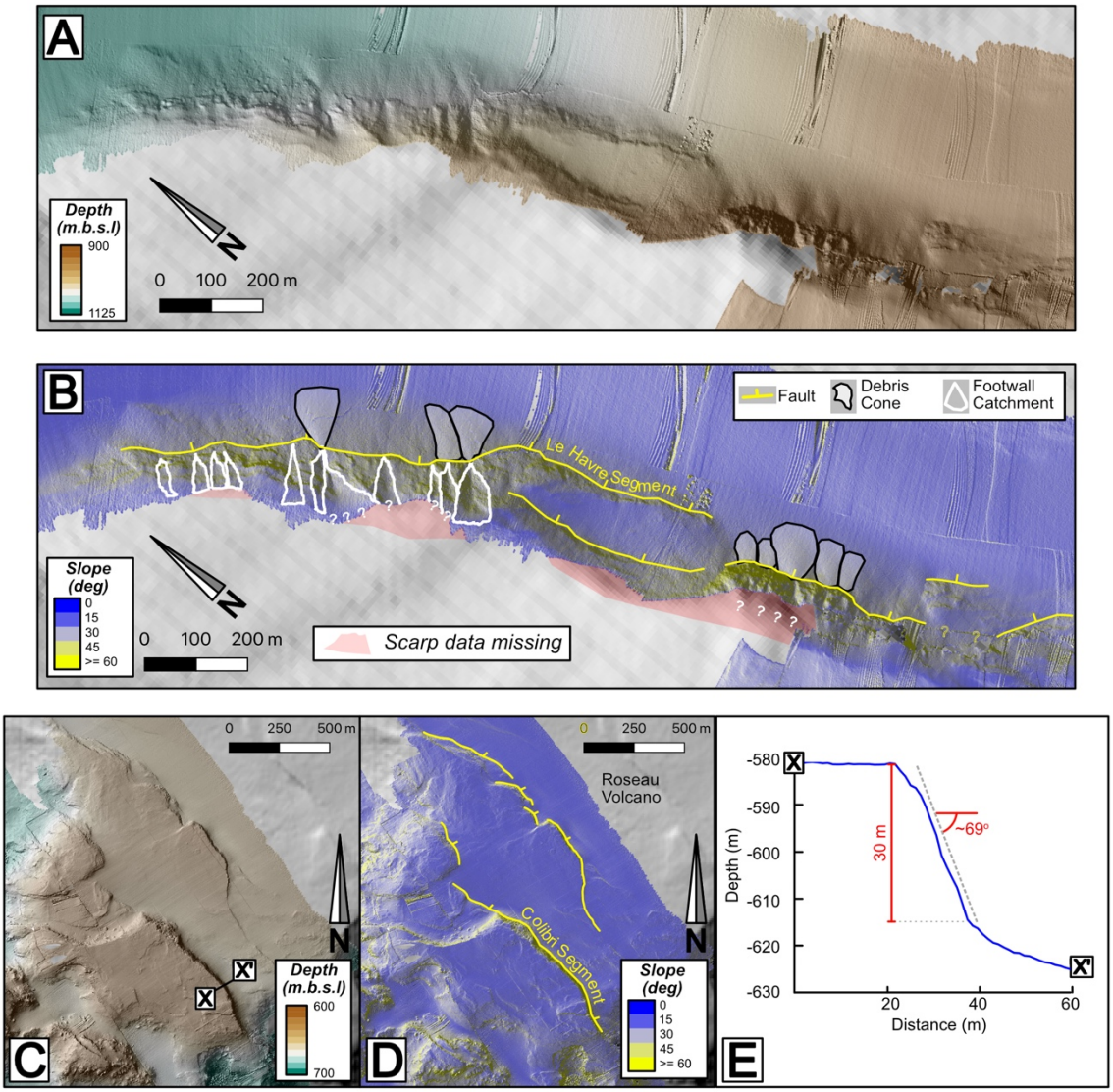

Figure S2. *Further examples of the morphology of the Roseau fault. The location of A and C are shown in Figure 3D. A) Shaded relief map from part of the Le Havre segment extracted from the 1 m/pixel digital terrain model (DTM) overlain on top of the 10 m/pixel DTM. B) Hillslope map of the same area as part A showing the interpretation of footwall catchments and debris cones associated with the Le Havre segment. These cones and catchments were not included in the volume balancing because data is missing from the 1 m/pixel DTM in the footwall to accurately quantify catchment volumes (red areas). C) Shaded relief map from the top of the Roseau volcano showing steep uneroded scarps up to 30 m tall that are associated with the Colibri segment. D) Hillslope map of the same area as part C with interpretation. E) Bathymetric profile X–X' (located in C) across the steep scarps in parts C and D.*

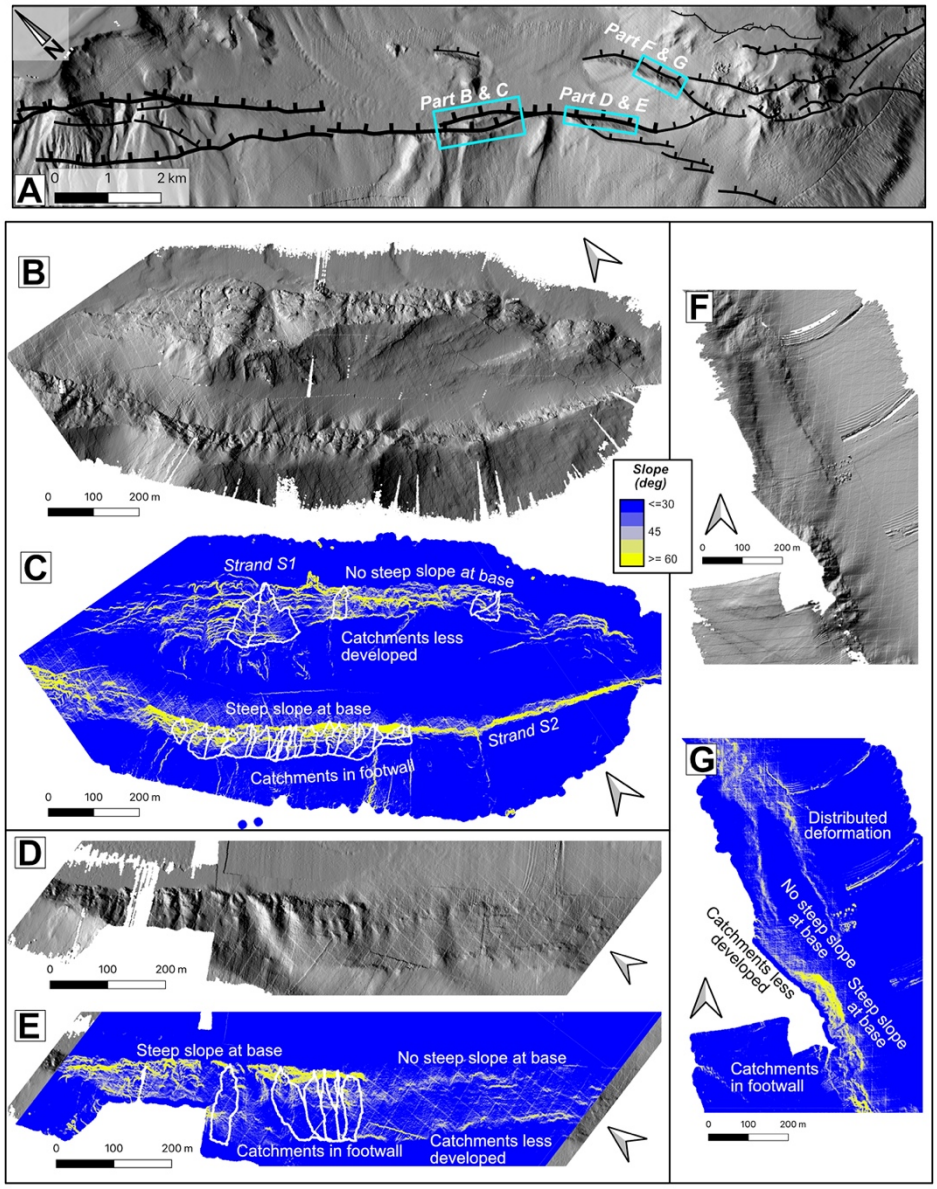

Figure S3. *Location of catchments in relation to high slope surfaces at the base of the scarp. A) Hillshade map showing location of parts B-G. Location of part A shown in Figure 4A. B) Hillshade map showing two strands of the Roseau segment (strand S1 and S2) with difference degrees of catchment development and slopes. C) Slope map of same area as B with interpretation. Catchments are delineated in white. D) Hill-shade map of the Roseau segment in area C showing pronounced catchments where a steep surface is present at the base of the scarp and much less pronounced catchments along strike where no steep surface is preserved at the base of the scarp. E) Slope map showing same area as D with interpretation. F) Hillshade map of the Le Havre segment showing pronounced catchments where a steep surface is present at the base of the scarp and no catchments along strike where no steep surface is preserved at the base of the scarp and deformation is distributed in two strands. G) Slope map from same area as part F with interpretation.*

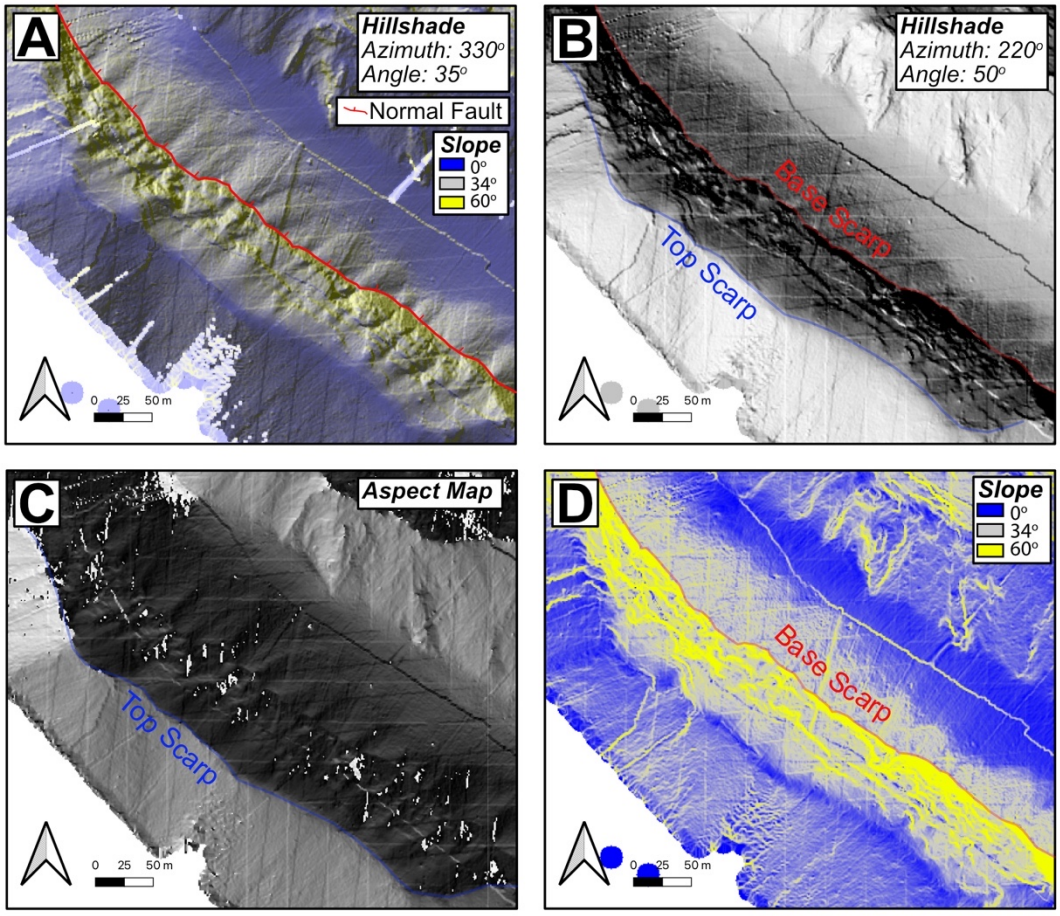

Figure S4. *Examples of how we used hillshade, aspect, and slope maps derived from the 1 m/pixel digital terrain model (DTM) to map the top and base of the scarp. A) Hillshade map with a light azimuth of 330° (from north) and a light angle of 35° (from horizontal) overlain by a transparent slope map with the mapped surface trace of strand S2 of the Roseau segment. The light angle of 330° is optimal for visualizing the morphology of debris cones and footwall catchments. B) Hillshade map with a light angle of 220° and a light azimuth of 50°. The light angle of 220° is oriented roughly perpendicular to fault strike and is directed from behind the footwall so that we can visualize both the drainage divide (the top of the scarp) and the hanging wall cut-off (the base of the scarp). C) Aspect map. Aspect is the facing direction of a slope for each pixel and ranges between 0–360°. Slopes facing north are shaded darker and slopes facing south are shaded lighter. We used aspect maps to delineate the top of the scarp. D) Slope map. Slope is measured as the angle from horizonal in degrees for each pixel. We capped the slope at 60° to highlight the steeply dipping (>60°) fault free face and show variation in slope below 60°. All maps show the same area located on Figure 3 of the main manuscript.*

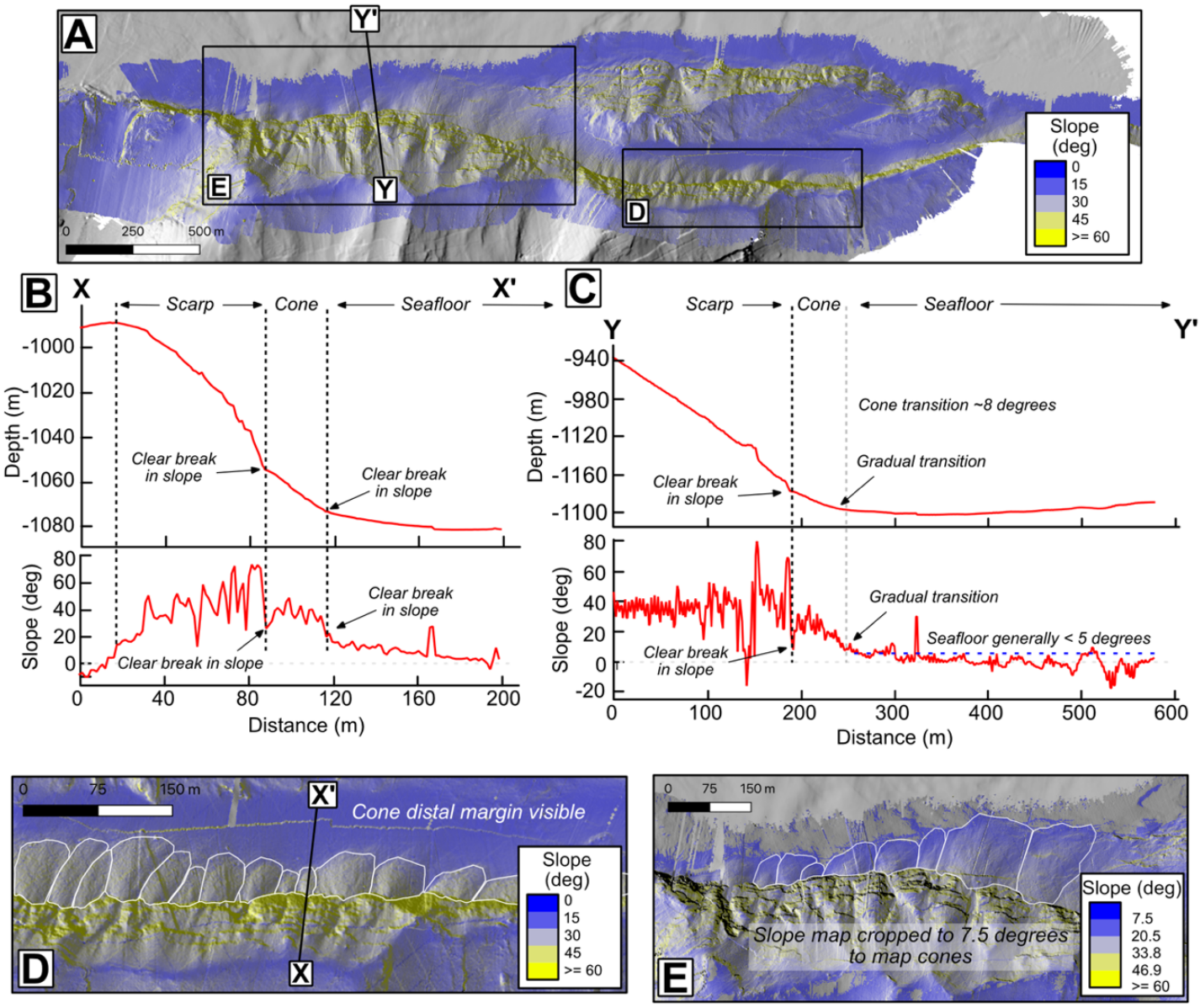

Figure S5. *Data used to quantify the distal boundaries of the cones. The location of part A is shown in Figure 3D. A) Hillslope map showing the location parts D and E. B) Section X–X' showing a cross section view of the clear break in slope between the base of the cone and the seafloor in the hanging wall. Line of section is in D. C) Section Y–Y' showing a gradual transition between the distal margin of the cone and the seafloor in the hanging wall. The slope profile also shows how the seafloor in the footwall generally dips less than 5° towards the fault, which indicates that the minimum slope of the cone surface should be slightly above 5°. D) Hillslope map from area B with minimum slope set to zero which shows how the distal margin of the cones is easy to trace without clipping the slope map due to a transition from yellow to blue. E) Hillslope map from area A with all pixels with slope less than 7.5° slope removed. 7.5° was selected because this is the minimum value above 5° that qualitatively produces a radial cone morphology to represent the distal margin of the cones.*

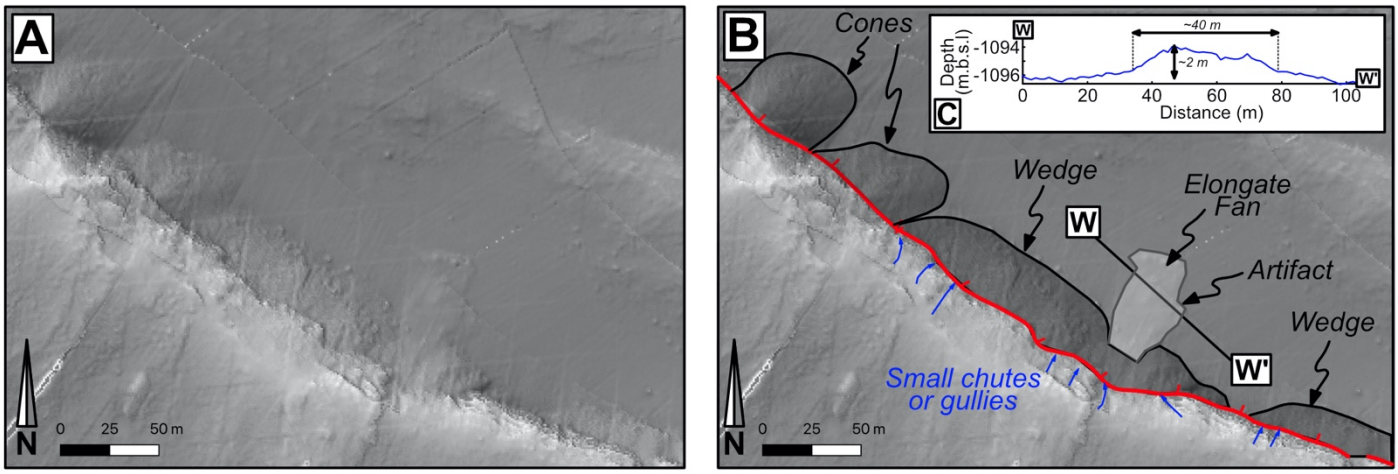

Figure S6. *A) Textured shaded relief map showing colluvial wedges at the base of the Roseau segment scarp. The location of parts A and B is shown in Figure 3D. B) Same image as A but with interpretation. Red line is surface trace of Roseau segment. Blue arrows are small gullies on the scarp surface. C) Bathymetric profile along the line W–W' across a low elongate fan.*

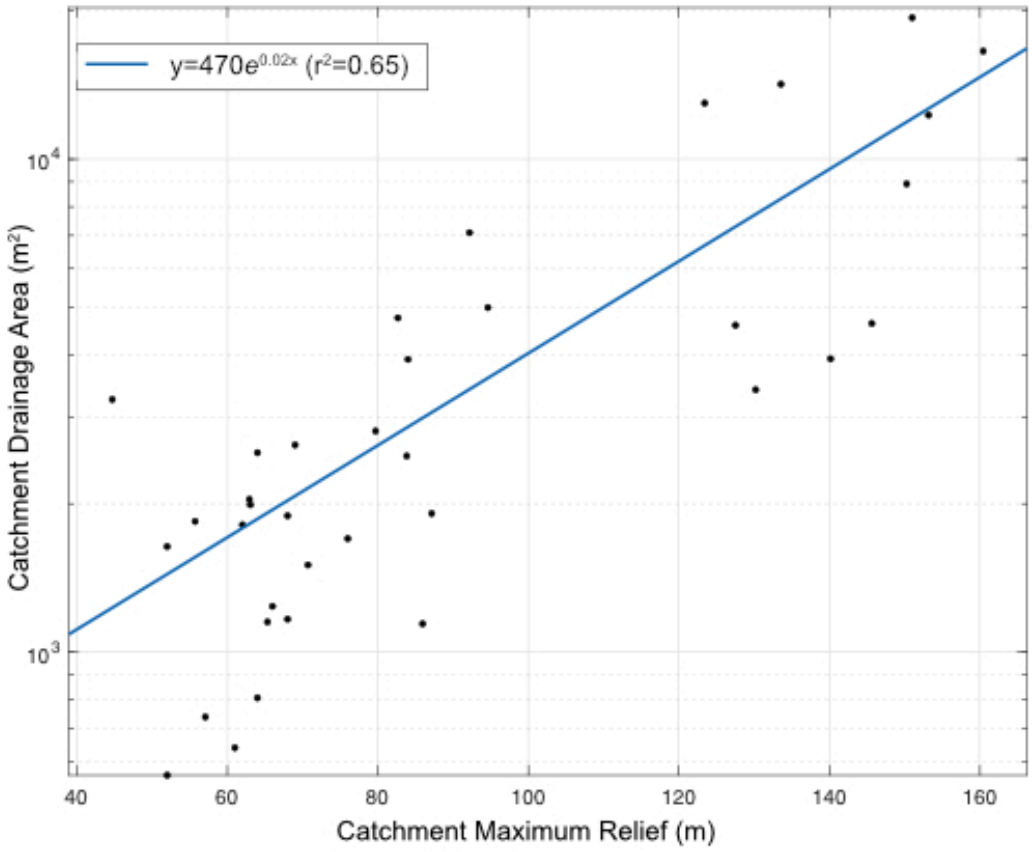

Figure S7. *Plot of catchment maximum relief versus catchment drainage area on a log-linear scale showing an exponential fit through the data.*

Cruise (Year)	***Device***	***Area***	***X Limit (°W)[c]***	***Y Limit (°N)[c]***	***Gridded DTM Resolution***
BATHYSAINTES (2010)	Multibeam systems RESON SEABAT 71111, RESON SEABAT 7150, and Kongsberg EM3002	Les Saintes plateau and Les Saintes channel	-61.8179–-613430	15.9659–15.5347	Datasets merged into a regional grid at 10 m/pixel
ODEMAR (2013)	200 kHz RESON SEABAT 7125 multibeam system onboard AUV Abyss [b]	~10 km^2 of the Roseau segment and the seafloor in the Roseau trough	-61.6145–-61.5668	15.7834–15.7384	2 m/pixel
	200 kHz RESON SEABAT 7125 multibeam system onboard ROV Victor6000 [a]	3.1 km^2 on Roseau segment and in hanging wall	-6160337–-6155592	15.76657–15.72248	0.5 m/pixel
	200 kHz RESON SEABAT 7125 multibeam system onboard ROV Victor6000 [a]	0.02 km^2 in hanging wall of Roseau segment	-61.58344–-61.58123	15.75016–15.74815	0.1 m/pixel
SUBSAINTES (2017)	Kongsberg Reson SMF EM2040 multibeam system onboard AUV Aster[x a]	~100 km^2 Across Les Saintes graben	-61.7127—61.3970	15.8716–15.6623	1 m/pixel

AUV = Autonomous underwater vehicle
ROV = Remotely operated vehicle
a= Ifremer, France
b= Geomar, Germany
c= WGS84 Geographic coordinates

Table S1. Summary of bathymetry data used in this study

ID	Model Name	UTM X	UTM Y	Depth	Dip Measured*	Average Dip (deg)+
1	653_NA	651606.5	1741848.7	-1066	0	-
2	653_NB	651886.9	1741661.8	-1050	0	-
3	654_jb11	651344.7	1742094.8	-1067	0	-
4	654_jb12	651332.5	1742110.0	-1065	1	86
5	654_jb17	650431.1	1743105.8	-986	0	-
6	654_FPA	651780.5	1741748.2	-1077	1	73
7	654_FPC	651696.4	1741804.6	-1082	1	71
8	654_FPD	651627.5	1741832.5	-1065	0	-
9	654_FPE	651419.4	1742020.1	-1068	1	69
10	654_FPF	651388.3	1742057.8	-1071	0	-
11	654_FPG	651358.4	1742077.5	-1066	1	62
12	654_FPQ	650912.1	1742550.4	-1027	0	-
13	653_654_jb16	651585.9	1741860.3	-1063	0	-
14	653_658_FPB	651818.3	1741728.5	-1076	1	73
15	654_658_AUTT18	651506.9	1741921.9	-1066	1	70
16	654_658_AUTT28	651264.2	1742165.2	-1062	0	-
17	654_658_NA	651010.9	1742460.1	-1045	0	-
18	654_658_NB	650472.1	1743065.7	-988	0	-
19	655_jb00	652645.4	1740900.6	-1073	0	-
20	655_jb01	652499.1	1741006.2	-1053	1	71
21	655_jb02	652319.5	1741145.6	-1012	1	72
22	655_jb03	652253.9	1741189.9	-995	1	-
23	655_jb04	652060.5	1741447.7	-1036	1	71
24	655_jb05	652015.3	1741512.3	-1052	1	76
25	655_jb06	652008.1	1741511.6	-1049	1	78
26	655_jb07	651955.4	1741596.0	-1061	0	-
27	655_jb08	652554.2	1741342.9	-1117	0	-
28	655_jb13	653074.0	1740733.6	-1098	0	-
29	655_jb14	653015.3	1740745.1	-1096	1	71
30	655_jb15	653265.1	1740649.8	-1132	0	-
31	655_AUTT66	651919.8	1741629.1	-1056	1	72
32	655_AUTTVT	653889.7	1739974.5	-1130	0	-
33	655_AUTT101	653278.7	1740660.8	-1133	0	-
34	658_AUTT12_C	649353.9	1744848.7	-795	0	-
35	658_B	650336.6	1743141.8	-966	0	-
36	658_FPN	651289.2	1742132.4	-1050	0	-
37	658_SBS_A	650366.4	1743135.4	-975	0	-
38	662_jb10	661564.8	1735992.0	-1241	0	-
39	663_AUTT12	648457.8	1746062.2	-612	0	-
40	663_AUTT17	648914.0	1745424.4	-743	0	-
41	666_jb09	655144.3	1738353.4	-907	0	-

1 = Dip measured from model, 0 = Dip not measured from model. See Figure S3 for map locations of models.
+ = Average dip is the average of between 1–8 individual measurements from each model.

Table S2. Data on three-dimensional outcrop models

Sample Name	IGSN	Field name (informal classification)	Classification	Latitude (°N)	Longitude (°W)	Elevation (mbsl)
SBS653_002	CNRS0000000901	Lava	igneous>volcanic	15.74959	-61.58326	-1075.64
SBS653_003	CNRS0000000902	Lava	igneous>volcanic	15.74961	-61.58331	-1074.67
SBS653_004	CNRS0000000903	Lava	igneous>volcanic	15.74951	-61.58342	-1049.25
SBS653_005	CNRS0000000904	Pyroclastic deposit	igneous>volcanic	15.74938	-61.58343	-1028.76
SBS653_006	CNRS0000000905	andesite	igneous>volcanic>intermediate	15.74864	-61.58395	-968.25
SBS653_007	CNRS0000000906	andesite	igneous>volcanic>intermediate	15.74854	-61.58399	-961.93
SBS653_008	CNRS0000000907	Pyroclastic deposit	igneous>volcanic>intermediate	15.74825	-61.58424	-935.23
SBS653_009	CNRS0000000908	Calcareous sandstone	sedimentary>carbonate	15.74827	-61.58425	-935.42
SBS653_010	CNRS0000000909	Fault rock	Metamorphic>mechanicallybroken	15.74887	-61.58236	-1070.49
SBS653_011	CNRS0000000910	Fault rock	Metamorphic>mechanicallybroken	15.74888	-61.58237	-1070.88
SBS654_013	CNRS0000000911	andesite	igneous>volcanic>intermediate	15.75099	-61.58558	-1059.6
SBS654_014	CNRS0000000912	andesite	igneous>volcanic>intermediate	15.75100	-61.58559	-1059.3
SBS654_015	CNRS0000000913	Fault gouge	Metamorphic>mechanicallybroken	15.75118	-61.58583	-1066.9
SBS654_016a-b	CNRS0000000914	cataclasite	Metamorphic>mechanicallybroken	15.75258	-61.58716	-1067.1
SBS654_016c	CNRS0000000915	andesite	igneous>volcanic>intermediate	15.75258	-61.58716	-1067.1
SBS654_017	CNRS0000000916	Calcareous sandstone	sedimentary>carbonate	15.75957	-61.59335	-1013.8
SBS654_018	CNRS0000000917	Calcareous sandstone	sedimentary>carbonate	15.75957	-61.59335	-1013.78
SBS654_019	CNRS0000000918	Volcaniclastic breccia	sedimentary>volcaniclastic	15.76024	-61.59448	-987.24
SBS654_020	CNRS0000000919	Volcaniclastic breccia	sedimentary>volcaniclastic	15.76201	-61.59682	-957.91
SBS654_021	CNRS0000000920	Volcaniclastic breccia	sedimentary>volcaniclastic	15.76195	-61.59718	-945.22
SBS655_022	CNRS0000000921	Volcaniclastic breccia	sedimentary>volcaniclastic	15.74806	-61.58161	-1057.8
SBS655_023	CNRS0000000922	Volcaniclastic breccia	sedimentary>volcaniclastic	15.74809	-61.58162	-1057.8
SBS655_024	CNRS0000000923	Volcaniclastic breccia	sedimentary>volcaniclastic	15.74809	-61.58162	-1058.3
SBS655_025	CNRS0000000924	Volcaniclastic breccia	sedimentary>volcaniclastic	15.74844	-61.58197	-1052.7
SBS655_026	CNRS0000000925	andesite	igneous>volcanic>intermediate	15.74878	-61.58226	-1062.6
SBS655_027	CNRS0000000926	sedimentary sandstone	sedimentary>volcaniclastic	15.74687	-61.57878	-1079.2
SBS655_028	CNRS0000000927	Volcaniclastic breccia	sedimentary>volcaniclastic	15.74690	-61.57748	-1115.1
SBS655_029	CNRS0000000928	Volcaniclastic breccia	sedimentary>volcaniclastic	15.74215	-61.57271	-1094
SBS655_030	CNRS0000000929	Sandstone	sedimentary	15.74215	-61.57271	-1094
SBS655_031	CNRS0000000930	Volcaniclastic breccia	sedimentary>volcaniclastic	15.73368	-61.56389	-1131.5
SBS655_032	CNRS0000000931	Volcaniclastic breccia	sedimentary>volcaniclastic	15.72677	-61.55940	-1064.9
SBS655_033	CNRS0000000932	dacite or welded ignimbrite	igneous>volcanic>felsic	15.73374	-61.55099	-976
SBS656_034	CNRS0000000933	dacite?	igneous>volcanic>intermediate	15.72866	-61.40562	-925.5
SBS656_035	CNRS0000000934	dacite ?	igneous>volcanic>intermediate	15.72819	-61.40684	-917.4
SBS656_036	CNRS0000000935	andesite	igneous>volcanic>intermediate	15.72958	-61.40698	-881
SBS656_037	CNRS0000000936	Sedimentary breccia	Sedimentary>ConglomerateAndOrBreccia	15.73236	-61.40733	-811
SBS656_038	CNRS0000000937	andesite	igneous>volcanic>intermediate	15.73351	-61.40737	-734

SBS656_039	CNRS0000000938	andesite	igneous>volcanic>intermediate	15.73355	-61.40732	-721
SBS656_040	CNRS0000000939	andesite	igneous>volcanic>intermediate	15.73362	-61.40717	-709.2
SBS656_041	CNRS0000000940	andesite	igneous>volcanic>intermediate	15.73369	-61.40705	-707.7
SBS656_042	CNRS0000000941	andesite	igneous>volcanic>intermediate	15.73278	-61.40911	-771.3
SBS656_043	CNRS0000000942	Calcareous sandstone	sedimentary>carbonate	15.73224	-61.41181	-751.8
SBS656_044	CNRS0000000943	andesite	igneous>volcanic>intermediate	15.73224	-61.41182	-750.8
SBS657_045	CNRS0000000944	Volcaniclastic breccia	sedimentary>volcaniclastic	15.72839	-61.41050	-1132
SBS657_046	CNRS0000000945	altered ava	igneous>volcanic>intermediate	15.72764	-61.41117	-1133
SBS657_047	CNRS0000000946	altered lava	igneous>volcanic>intermediate	15.72891	-61.41124	-1134
SBS657_048	CNRS0000000947	andesite	igneous>volcanic>intermediate	15.72932	-61.41126	-1135
SBS657_049	CNRS0000000948	lava	igneous>volcanic>intermediate	15.73011	-61.41198	-1136
SBS657_050	CNRS0000000949	welded lava flow	igneous>volcanic>intermediate	15.73306	-61.41464	-1137
SBS657_051	CNRS0000000950	carbonate breccia	Sedimentary>ConglomerateAndOrBreccia	15.73830	-61.41566	-1138
SBS657_052	CNRS0000000951	sedimentary sandstone	sedimentary>carbonate	15.73857	-61.41578	-1139
SBS657_053	CNRS0000000952	Sedimentary breccia	Sedimentary>ConglomerateAndOrBreccia	15.74021	-61.41671	-1140
SBS657_054	CNRS0000000953	Lava	igneous>volcanic	15.74335	-61.41655	-1141
SBS657_055	CNRS0000000954	Lava	igneous>volcanic	15.74335	-61.41653	-1142
SBS658_056	CNRS0000000955	volcaniclastic Breccia	sedimentary>volcaniclastic	15.76286	-61.59738	-956
SBS658_057	CNRS0000000956	volcaniclastic Breccia	sedimentary>volcaniclastic	15.76902	-61.60533	-693
SBS658_058	CNRS0000000957	limestone	sedimentary>carbonate	15.77767	-61.60559	-795
SBS659_059	CNRS0000000958	amphible-riche dacite	igneous>volcanic>intermediate	15.75147	-61.47676	-660
SBS659_060	CNRS0000000959	amphible-riche dacite	igneous>volcanic>intermediate	15.75161	-61.47641	-637
SBS659_061	CNRS0000000960	amphible-riche dacite	igneous>volcanic>intermediate	15.75161	-61.47563	-598
SBS659_062	CNRS0000000961	amphible-riche dacite	igneous>volcanic>intermediate	15.75063	-61.47548	-633
SBS659_063	CNRS0000000962	amphible-riche dacite	igneous>volcanic>intermediate	15.75062	-61.47546	-635
SBS659_064	CNRS0000000963	vitric lava	igneous>volcanic>felsic	15.75064	-61.47569	-632
SBS659_065	CNRS0000000964	vitric lava	igneous>volcanic>felsic	15.75064	-61.47570	-632
SBS659_066	CNRS0000000965	sandstone, pyroclastic deposit ?	igneous>volcanic	15.75100	-61.47908	-713
SBS659_067	CNRS0000000966	andesite clast from volcanic breccia	igneous>volcanic>intermediate	15.75233	-61.48050	-715
SBS659_068	CNRS0000000967	bread crust lava bomb	igneous>volcanic	15.75379	-61.47877	-722
SBS659_069	CNRS0000000968	welded ignimbrite?	igneous>volcanic>felsic	15.75566	-61.47854	-664
SBS659_070	CNRS0000000969	clast from a pyroclastic deposit ?	igneous>volcanic>intermediate	15.75700	-61.47944	-602
SBS659_071	CNRS0000000970	amphible-riche dacite	igneous>volcanic>intermediate	15.75829	-61.47945	-595
SBS659_072	CNRS0000000971	amphible-riche dacite	igneous>volcanic>intermediate	15.75238	-61.47590	-666
SBS659_073	CNRS0000000972	amphible-riche dacite	igneous>volcanic>intermediate	15.75183	-61.47498	-652
SBS659_074	CNRS0000000973	amphible-riche dacite	igneous>volcanic>intermediate	15.75138	-61.47471	-655
SBS659_075	CNRS0000000974	amphible-riche dacite	igneous>volcanic>intermediate	15.75154	-61.47543	-594
SBS659_076	CNRS0000000975	amphible-riche dacite	igneous>volcanic>intermediate	15.75149	-61.47543	-592

SBS659_077	CNRS0000000976	amphible-riche dacite	igneous>volcanic>intermediate	15.75147	-61.47546	-588
SBS659_078	CNRS0000000977	amphible-riche dacite	igneous>volcanic>intermediate	15.75143	-61.47556	-585
SBS659_079	CNRS0000000978	amphible-riche dacite	igneous>volcanic>intermediate	15.75132	-61.47569	-577
SBS660_080	CNRS0000000979	bedded bio and volcaniclastic deposit	sedimentary>volcaniclastic	15.73833	-61.48950	-904
SBS660_081	CNRS0000000980	basaltic andesite	igneous>volcanic>intermediate	15.73934	-61.48839	-857
SBS660_082	CNRS0000000981	basaltic andesite	igneous>volcanic>intermediate	15.73911	-61.48865	-859
SBS660_083	CNRS0000000982	basaltic andesite	igneous>volcanic>intermediate	15.73948	-61.48888	-855
SBS660_084	CNRS0000000983	lava	igneous>volcanic	15.73993	-61.48919	-862
SBS660_085	CNRS0000000984	lava with plutonic xenoliths	xenolithic>igneous>plutonic>mafic	15.73846	-61.48935	-893
SBS660_086	CNRS0000000985	volcaniclastic sandstone	sedimentary>volcaniclastic	15.74076	-61.48709	-863
SBS660_087	CNRS0000000986	andesite	igneous>volcanic>intermediate	15.73681	-61.48420	-894
SBS660_088	CNRS0000000987	Volcaniclastic breccia	sedimentary>volcaniclastic	15.75520	-61.47310	-635
SBS660_089	CNRS0000000988	Volcaniclastic breccia	sedimentary>volcaniclastic	15.76808	-61.47810	-638
SBS660_090	CNRS0000000989	iron concretion	hydrothermal>oxide	15.76962	-61.47920	-628
SBS660_091	CNRS0000000990	iron concretion	Hydrothermal>oxide	15.76991	-61.48081	-646
SBS660_092	CNRS0000000991	iron concretion	hydrothermal>oxide	15.76965	-61.48006	-631
SBS660_093	CNRS0000000992	iron concretion	Hydrothermal>oxide	15.76955	-61.47912	-627
SBS660_094	CNRS0000000993	calcareous breccia	Sedimentary>ConglomerateAndOrBreccia	15.77101	-61.48025	-630
SBS660_095	CNRS0000000994	bedded sandstone with volcanic fragments	sedimentary>volcaniclastic	15.77148	-61.48064	-621
SBS660_096	CNRS0000000995	sandstone with volcanic fragments	sedimentary>volcaniclastic	15.77165	-61.48100	-627
SBS661_097	CNRS0000000996	dacite	igneous>volcanic>intermediate	15.67723	-61.46269	-509.32
SBS661_098	CNRS0000000997	dacite	igneous>volcanic>intermediate	15.67570	-61.46479	-326.14
SBS661_099	CNRS0000000998	lava	igneous>volcanic>intermediate	15.67569	-61.46485	-374.45
SBS661_100	CNRS0000000999	lava clasts from volcaniclastic breccia	sedimentary>volcaniclastic	15.67455	-61.46560	-257.42
SBS661_101	CNRS0000001000	lava clasts from volcaniclastic breccia	sedimentary>volcaniclastic	15.67499	-61.46546	-260.36
SBS661_102	CNRS0000001001	lava clast	igneous>volcanic>intermediate	15.67530	-61.46553	-270.97
SBS661_103	CNRS0000001002	dacite	igneous>volcanic>intermediate	15.67573	-61.46606	-250.1
SBS661_104	CNRS0000001003	lava	igneous>volcanic	15.67606	-61.46599	-266.39
SBS661_105	CNRS0000001004	andesite	igneous>volcanic>intermediate	15.67709	-61.46574	-342.84
SBS661_107	CNRS0000001005	porphyritic lava	igneous>volcanic	15.67415	-61.47209	-307.32
SBS661_108	CNRS0000001006	porphyritic lava	igneous>volcanic	15.67417	-61.47211	-307
SBS661_109	CNRS0000001007	porphyritic lava	igneous>volcanic	15.67619	-61.47225	-334
SBS661_110	CNRS0000001008	lava	igneous>volcanic	15.67649	-61.47274	-327
SBS661_111	CNRS0000001009	porphyritic lava	igneous>volcanic	15.67798	-61.47689	-436
SBS661_112	CNRS0000001010	porphyritic lava	igneous>volcanic	15.67719	-61.47580	-337
SBS661_113	CNRS0000001011	andesite	igneous>volcanic>intermediate	15.67565	-61.47593	-257
SBS661_114	CNRS0000001012	dacite	igneous>volcanic>intermediate	15.67496	-61.47709	-266
SBS661_115	CNRS0000001013	lava with plutonic xenoliths	xenolithic>igneous>plutonic>mafic	15.67501	-61.47710	-272

SBS661_116	CNRS0000001014	highly porphyritic lava	igneous>volcanic>intermediate	15.67436	-61.47704	-222
SBS661_117	CNRS0000001015	dacite	igneous>volcanic>intermediate	15.67701	-61.48107	-477
SBS661_118	CNRS0000001016	dacite	igneous>volcanic>intermediate	15.67712	-61.48144	-504
SBS661_119	CNRS0000001017	dacite	igneous>volcanic>intermediate	15.67716	-61.48176	-536
SBS661_120	CNRS0000001018	dacite	igneous>volcanic>intermediate	15.67778	-61.48274	-638
SBS661_121	CNRS0000001019	dacite	igneous>volcanic>intermediate	15.68057	-61.48198	-742
SBS661_122	CNRS0000001020	very porous lava clast	igneous>volcanic	15.68085	-61.48142	-747
SBS662_123	CNRS0000001021	sedimentary sandstone	sedimentary	15.70162	-61.48657	-1183
SBS662_124	CNRS0000001022	sedimentary sandstone	sedimentary	15.70124	-61.48625	-1177
SBS662_125	CNRS0000001023	lava	igneous>volcanic	15.70102	-61.48679	-1214
SBS662_126	CNRS0000001024	lava clast from volcaniclastic deposit	igneous>volcanic	15.70052	-61.48722	-1180
SBS662_127	CNRS0000001025	lava	igneous>volcanic	15.69671	-61.49234	-1236
SBS662_128	CNRS0000001026	lava clast from volcaniclastic breccia	sedimentary>volcaniclastic	15.69573	-61.49364	-1226
SBS662_129	CNRS0000001027	massive lava	igneous>volcanic	15.69123	-61.49562	-1262
SBS662_130	CNRS0000001028	pyroclastic deposit, pumice	igneous>volcanic>felsic	15.69772	-61.50380	-1230
SBS662_131	CNRS0000001029	pyroclastic deposit	igneous>volcanic>felsic	15.69771	-61.50382	-1229
SBS662_132	CNRS0000001030	massive lava	igneous>volcanic	15.69772	-61.50381	-1229
SBS662_133	CNRS0000001031	massive lava	igneous>volcanic	15.69858	-61.50497	-1203
SBS662_134	CNRS0000001032	Volcaniclastic breccia	sedimentary>volcaniclastic	15.69903	-61.50602	-1185
SBS662_135	CNRS0000001033	massive lava	igneous>volcanic	15.70214	-61.50403	-1179
SBS662_136	CNRS0000001034	massive lava	igneous>volcanic	15.70307	-61.50387	-1092
SBS662_137	CNRS0000001035	massive lava	igneous>volcanic	15.70535	-61.50509	-1092
SBS662_138	CNRS0000001036	lava with fluidal texture	igneous>volcanic	15.70527	-61.50753	-1089
SBS662_139	CNRS0000001037	massive lava	igneous>volcanic	15.70640	-61.50581	-1030
SBS662_140	CNRS0000001038	massive lava	igneous>volcanic	15.70849	-61.50636	-1084
SBS662_141	CNRS0000001039	massive lava	igneous>volcanic	15.70965	-61.50969	-1000
SBS662_142	CNRS0000001040	massive lava	igneous>volcanic	15.71132	-61.51302	-912
SBS662_143	CNRS0000001041	welded ignimbrite ?	igneous>volcanic>felsic	15.71724	-61.51660	-714
SBS662_144	CNRS0000001042	volcaniclastic breccia	sedimentary>volcaniclastic	15.71781	-61.51668	-696
SBS662_145	CNRS0000001043	dacite clast from volcaniclastic breccia	igneous>volcanic>intermediate	15.72168	-61.52354	-614
SBS662_146	CNRS0000001044	dacite clast from volcaniclastic breccia	igneous>volcanic>intermediate	15.72292	-61.52457	-610
SBS662_147	CNRS0000001045	dacite clast from volcaniclastic breccia	igneous>volcanic>intermediate	15.72632	-61.52451	-519
SBS662_148	CNRS0000001046	volcanic bomb, dacite	igneous>volcanic>intermediate	15.72456	-61.52411	-569
SBS662_149	CNRS0000001047	volcanic bomb	igneous>volcanic	15.72296	-61.52431	-570
SBS662_150	CNRS0000001048	amphibole-rich massive lava	igneous>volcanic>intermediate	15.74013	-61.52163	-525
SBS662_151	CNRS0000001049	massive lava	igneous>volcanic>intermediate	15.74807	-61.52145	-707
SBS662_152	CNRS0000001050	massive lava	igneous>volcanic>intermediate	15.74870	-61.52127	-678
SBS662_153	CNRS0000001051	iron concretion	Hydrothermal>oxide	15.71948	-61.52033	-612

SBS663_154	CNRS0000001052	dacite ?	igneous>volcanic>intermediate	15.82237	-61.65093	-319
SBS663_156	CNRS0000001053	lava	igneous>volcanic>intermediate	15.80836	-61.64047	-531
SBS663_157	CNRS0000001054	lava	igneous>volcanic>intermediate	15.80622	-61.63604	-554
SBS663_158	CNRS0000001055	andesite	igneous>volcanic>intermediate	15.79899	-61.62705	-347
SBS663_159	CNRS0000001056	lava	igneous>volcanic>intermediate	15.77238	-61.54124	-811
SBS663_160	CNRS0000001057	pyroclastic deposit from tuff cone	igneous>volcanic	15.77365	-61.53968	-754
SBS663_161	CNRS0000001058	lava	igneous>volcanic>intermediate	15.77597	-61.53372	-642
SBS663_162	CNRS0000001059	lava	igneous>volcanic>intermediate	15.77404	-61.53100	-591
SBS663_163	CNRS0000001060	lava	igneous>volcanic>intermediate	15.77445	-61.53035	-619
SBS664_164	CNRS0000001061	lava clast from volcaniclastic breccia	igneous>volcanic>intermediate	15.73825	-61.52187	-529
SBS664_165	CNRS0000001062	tuffaceous carbonate concretion	sedimentary>carbonate	15.73849	-61.52183	-526
SBS664_166	CNRS0000001063	massive lava	igneous>volcanic>intermediate	15.74078	-61.52129	-549
SBS664_167	CNRS0000001064	lava	igneous>volcanic>intermediate	15.74173	-61.52277	-559
SBS664_168	CNRS0000001065	tuffaceous carbonate concretion	sedimentary>carbonate	15.74148	-61.52352	-546
SBS664_169	CNRS0000001066	lava	igneous>volcanic>intermediate	15.73993	-61.52274	-497
SBS664_170	CNRS0000001067	lava	igneous>volcanic>intermediate	15.74128	-61.52143	-555
SBS664_171	CNRS0000001068	lava	igneous>volcanic>intermediate	15.75014	-61.52077	-688
SBS664_172	CNRS0000001069	tuffaceous carbonate concretion	sedimentary>carbonate	15.75091	-61.52033	-694
SBS664_173	CNRS0000001070	lava	igneous>volcanic>intermediate	15.74907	-61.52267	-704
SBS664_174	CNRS0000001071	lava	igneous>volcanic>intermediate	15.74865	-61.52104	-680
SBS664_175	CNRS0000001072	volcaniclastic breccia	sedimentary>volcaniclastic	15.74746	-61.51576	-747
SBS664_176	CNRS0000001073	lava	igneous>volcanic>intermediate	15.74723	-61.51706	-755
SBS664_177	CNRS0000001074	volcaniclastic breccia	sedimentary>volcaniclastic	15.74760	-61.51722	-755
SBS664_178	CNRS0000001075	carbonaceous breccia	sedimentary>carbonate	15.75158	-61.52302	-698
SBS664_179	CNRS0000001076	lava	igneous>volcanic>intermediate	15.77024	-61.53415	-740
SBS664_180	CNRS0000001077	lava	igneous>volcanic>intermediate	15.76900	-61.52827	-758
SBS664_181	CNRS0000001078	volcaniclastic breccia	Sedimentary>ConglomerateAndOrBreccia	15.76926	-61.52878	-726
SBS664_182	CNRS0000001079	lava	igneous>volcanic>intermediate	15.77365	-61.53079	-603
SBS664_183	CNRS0000001080	lava	igneous>volcanic>intermediate	15.77402	-61.53084	-596
SBS664_184	CNRS0000001081	sedimentary sandstone	sedimentary	15.77341	-61.53269	-649
SBS664_185	CNRS0000001082	lava	igneous>volcanic>intermediate	15.77392	-61.53391	-666
SBS664_186	CNRS0000001083	lava	igneous>volcanic>intermediate	15.77696	-61.53702	-787
SBS664_187	CNRS0000001084	lava	igneous>volcanic>intermediate	15.77526	-61.53822	-785
SBS664_188	CNRS0000001085	lava	igneous>volcanic>intermediate	15.77360	-61.54388	-823
SBS664_189	CNRS0000001086	tuffaceous carbonate concretion	sedimentary>carbonate	15.77530	-61.54624	-830
SBS664_190	CNRS0000001087	lava	igneous>volcanic>intermediate	15.77794	-61.55019	-695
SBS665_191	CNRS0000001088	ruggy concretion, probably silica	sedimentary	15.79737	-61.48089	-412
SBS665_192	CNRS0000001089	sedimentary sandstone	sedimentary	15.79715	-61.48039	-414

SBS665_193	CNRS0000001090	sedimentary sandstone	sedimentary	15.78922	-61.47922	-571
SBS665_194	CNRS0000001091	volcanoclastic breccia	sedimentary>volcaniclastic	15.78296	-61.47422	-578
SBS665_195	CNRS0000001092	iron concretion	ore>oxide	15.77863	-61.47077	-589
SBS665_196	CNRS0000001093	laminated sedimentary siltstone	sedimentary	15.77795	-61.46958	-564
SBS665_197	CNRS0000001094	laminated sedimentary siltstone	sedimentary	15.77819	-61.46693	-441
SBS666-198	CNRS0000001095	Pyroclastic deposit, pumice	igneous>volcanic>felsic	15.69769	-61.50382	-1230
SBS666-199	CNRS0000001096	pyroclastic deposit , pumice	igneous>volcanic>felsic	15.69794	-61.50395	-1229
SBS666-200	CNRS0000001097	pyroclastic deposit, pumice	igneous>volcanic>felsic	15.69772	-61.50385	-1228
SBS666-201	CNRS0000001098	pyroclastic deposit and carbonaceous sandstone	igneous>volcanic	15.71445	-61.53925	-644
mbsl = Meters below seal level						

Table S3. Summary of rock sample collected using the remotely operated vehicle.

Basin Id*	Drainage Area (m^2)	Max Relief (m)	Mean Gradient (deg)
		Area A	
1	3936	140	43
2	4602	128	50
3	4643	146	37
4	19354	151	35
5	12285	153	30
6	8907	150	45
7	16557	160	36
8	3407	130	39
9	14188	134	35
10	12987	123	38
		Area B: Strand S2	
11	1152	65	52
12	2042	63	40
13	1991	63	42
14	739	57	50
15	2632	69	36
16	1842	56	35
16a	640	61	37
17	1239	66	35
18	808	64	37
19	1891	68	42
20	1700	76	39
21	1167	68	40
22	1813	62	36
23	563	52	40
24	2539	64	34
25	1638	52	37
		Area C	
26	3925	84	34
27	4763	83	32
28	2500	84	32
29	1911	87	30
30	1142	86	31
31	2809	80	37
		Area B: Strand S1	
32	4999	95	37
33	7092	92	36
34	1503	71	46
35	3255	45	28

**Id refers to numerical identifiers on Figure 5c*

Table S4. Data on catchment drainage area, catchment mean gradient, and maximum relief used in Figure 11a and 11b.

Basin id [A]	Basin Volume (m^3) +/-		Drainage Area (m^2)	Max Height (m)[B]	Cone Volume (m^3) +/-		Cone Ave. Surface Slope (deg)	Hanging wall deposition /Footwall erosion (V_{HW}/V_{FW})
			Area a					
1'	*119360*	*67758 / 54651*	*3936*	*140*	*1281*	*173 / 192*	*22*	0.01
2'	*137208*	*63463 / 51538*	*4602*	*128*	*20266*	*3033 / 3282*	*23*	0.15
3	107656	46435 / 35835	4643	146	11930	8182 / 8096	19	0.11
4	812373	325293 / 246127	19354	151	15149	10049 / 9903	18	0.02
5	621457	245564 / 183485	12285	153	2259	1564 / 1536	15	0.00
6	307805	122972 / 95400	8907	150	21210	16107 / 1585	16	0.07
7	730719	285326 / 218531	16557	160	26052	18316 / 18068	17	0.04
8	82172	40987 / 32506	3407	130	18051	14888 / 14618	15	0.22
9	669375	244325 / 185230	14188	134	295909	174689 / 174378	23	0.44
10	514106	209154 / 163094	12987	123	278357	154247 / 154187	21	0.54
			Area B					
11	16113	10835 / 9145	1152	65	17630	7907 / 8066	31	1.09
12	34098	15970 / 12487	2042	63	35121	15423 / 15755	31	1.03
13	29218	15333 / 12313	1991	63	19125	8256 / 8401	28	0.65
14	5374	3624 / 3030	739	57	12574	5196 / 5304	31	2.34
15	35337	14587 / 11298	2632	69	37070	16359 / 16578	26	1.05
16	27477	12461 / 9680	1842	56	15440	6542 / 6648	30	0.56
16a	5508	2413 / 1890	640	61	6335	2839 / 2899	32	1.15
17,18	35433	16493 / 12910	2047	66	17863	8322 / 8443	29	0.50
19	26978	16288 / 13029	1891	68	10290	4957 / 4999	26	0.38
20	22385	14457 / 11529	1700	76	1808	825 / 836	28	0.08
21	14072	7939 / 6270	1167	68	2756	1248 / 1269	30	0.20
22,23	31987	15135 / 11827	2376	62	20419	9788 / 9926	29	0.64
24	32388	13992 / 10776	2539	64	12773	6508 / 6522	23	0.39
25	7928	4011 / 3185	1638	52	8505	4159 / 4202	27	1.07
*	-	-	-	-	18611	8625 / 8868	34	
*	-	-	-	-	5687	2453 / 2525	34	
*	-	-	-	-	5754	2602 / 2662	32	
			Area C					
26	126426	47159 / 35937	3925	84	150	87 / 86	19	0.00
26a+	-	-	-	-	1135	797 / 781	14	
27	74688	21746 / 16846	4763	83	116	115 / 113	16	0.00
28	42371	14932 / 12170	2500	84	461	232 / 232	24	0.01
29	30896	11085 / 9023	1911	87	166	93 / 93	21	0.01
30	22557	8034 / 6591	1142	86	352	218 / 216	19	0.02
31	77199	26760 / 22373	2809	80	1913	1086 / 1080	21	0.02

A: Basin ID refers to catchments on Figure 5
B: Max height is measured from the top of the material deposited in the hanging wall.
' High-resolution bathymetry data is missing from parts of the surface of cones adjacent to catchments 1 and 2 so these cones were not considered in our analysis.
** There are no well-developed catchment in the footwall which correspond to these steep cones.*
+There is a large footwall catchment corresponding to this catchment but the headward boundary of the catchment is not clear.

Table S5. Data on footwall catchments and associated dejection cones presented in Figure 11c